MODELLING OF CONSTRICTION PHENOMENON IN COMPOSITE CONTAINING CONDUCTIVE CARBON PARTICLES

Ivana PILARČÍKOVÁ, Josef HAMPL, Slavomír JIRKŮ

Authors: **_Ivana Pilarčíková, MSc., Josef Hampl, PhD., Ing. Slavomír Jirků, Assoc. Prof., PhD._**
Workplace: **_České vysoké učení technické v Praze, Fakulta elektrotechnická_**
Adress: **_Technická 2, 166 27 Praha 6, Czech Republic_**
Phone: **_+420 22435 2057_**
E-mail: **_pilarcik@fel.cvut.cz, ej.hampl@seznam.cz, jirku@fel.cvut.cz_**

Abstract

Solution of constriction phenomenon in polymer composites filled with conductive carbon particles is presented it this paper. Constriction phenomenon in polymer composites filled with conductive carbon particles is solved in plane at use of two models.

1st Model: Contact of spherical particles. It is assumed that carbon particles in composites can not only contact each other (as metals) but also grow through each other.

2nd Model: Connecting of two spherical particles by means of conductive bridge.

The two models of carbon particles connection show the electric field shape and electric resistance of the carbon particle/insulating matrix system.

Key words

polymer composites, carbon black, modelling, constriction phenomenon, resistivity, contact of conductive particles

Introduction

Solution of constriction phenomenon in polymer composites filled with conductive carbon particles is based on theory of contacts transient resistance [2].

A **contact** represents two electrical conductors being in common contact. Through these conductors, electric current is flowing at contact points. Since surface of no contact is absolutely flat, electric current flows from one contact to another only at certain points (Fig. 1). This effect (called constriction phenomenon) represents one of main causes of contacts transient resistance.

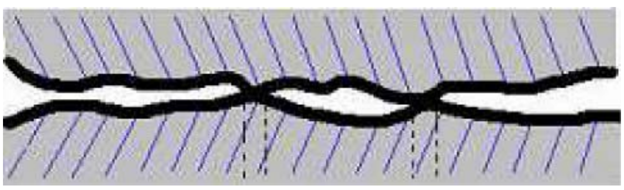

Fig. 1 *Contact points of conductors*

Proper contact points of printed contacts represent only a minor part of total contact surface. Inputting into the so called constriction point, current lines narrow themselves and the current flows only through a small contact surface. A constriction space is of certain active resistance. Its amount is determined for pure metals in vacuum. If some electric current flows through the constriction space, the following voltage within the so called R_{CR} constriction resistance originates

$$U_{CR} = R_{CR} \cdot I \; . \tag{1}$$

If a cylindrical conductor of *L* length is considered, some voltage drop on R_0 resistor occurs at *I* current flow through the conductor. If the conductor is mechanically divided and newly originated parts are put together again, a small *S* contact surface forms, at concurrence of *F* compressive force, in the conductor centre (Fig. 2). Voltage drop within the conductor of the same length and including a break point increases from U_0 to *U* because total resistance increased to

$$R = R_0 + R_{CR} \, , \tag{2}$$

$$U = I \cdot \left(R_0 + R_{CR}\right). \tag{3}$$

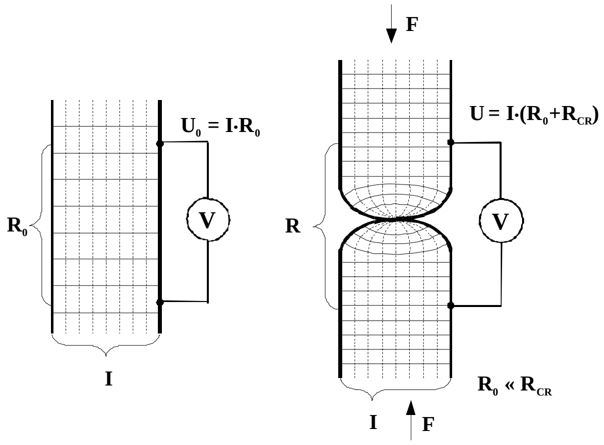

Fig. 2 *Current lines process and equipotential lines within conductor and contact constriction proximity*

Certainly, measuring of transient resistance value amount represents the simplest method of its detection. It can be realized by means of a number of more or less exact methods (V-A method, Thomson bridge, etc.).

Solving

Constriction phenomenon in polymer composites filled with conductive carbon particles is solved in a plane at use of two models.

1st Model: Contact of spherical particles

It is assumed that carbon particles in composites can not only contact each other (as metals) but also grow through each other [1, 3].

D particle diameter
d overlay length
$R_{\square}$ conductive paper square resistance
$R'_{\square}$ conductive electrodes square resistance

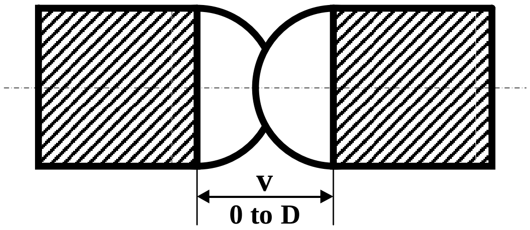

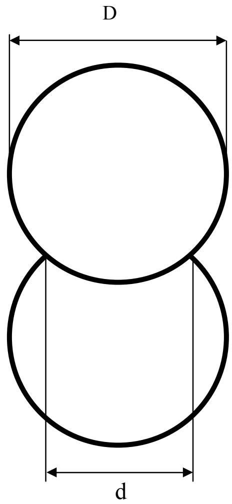

Fig. 3 *Contact of spherical particles*

Cross-hatched surface is of high-conductive varnish and $R'_{\square} = 10^{-4} R_{\square}$, semicircular segment of conductive paper is of ρ resistivity. Electrode contact is of *D* width while particle one of *d* width. The *v* value varies from 0 to *D*.

D and *d* widths match with overlay of both particles.

By measuring on the model (Fig. 3), distribution of current field within the semicircular segment as well as shape resistance arisen from field deformation are detected.

2nd Model: Connecting of two spherical particles by means of conductive bridge [1, 3]
D particle diameter, *w* bridge width, *l* bridge length.
Bridge surface is the same as spherical particle cross-section:

$$l \cdot w = \pi \frac{D^2}{4}. \quad (4)$$

Particle and bridge resistivities are of square resistance $R_{\square}$.

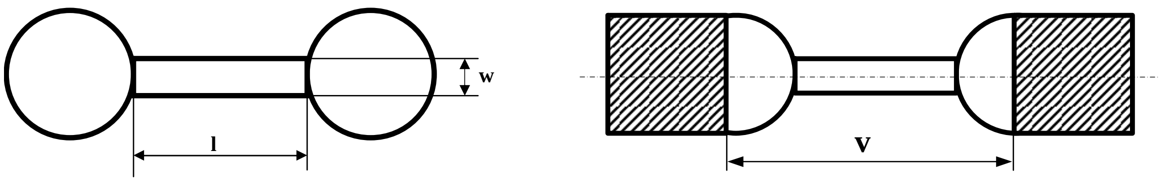

Fig. 4 *Connecting of two spherical particles by means of conductive bridge*

Cross-hatched surface is of high-conductive varnish and $R'_{\square} = 10^{-4} R_{\square}$, semicircular segment and bridge are of conductive paper and $R_{\square}$ resistance. Semicircular segment is of *D* diameter.

Graphite bridge is of *w*×*l* sizes and $R_{\square}$ resistance.

By measuring on the model (Fig. 4), distribution of current field within the semicircular segment as well as shape resistance arisen from field deformation are detected. Bridge slenderness changes during measuring.

Model conductive environment

For realization of planar field analogous model, it is used direct current field in a layer of graphite paper of constant h thickness.

Aside from model site, supply voltage or current is also affected by ρ specific resistance of used environment and its dependence on temperature or current density.

In this case, the layer thickness h is not exactly known and, therefore, so called $R_{\square}$ square resistance is introduced in place of ρ specific resistance [6]. It represents square resistance of sample of h thickness and arbitrary a side length:

$$R_{\square} = \rho \frac{a}{a \cdot h} = \frac{\rho}{h} \tag{5}$$

$R_{\square}$ is measured on rectangle band of l length and b width with connected conductive electrodes. If U is voltage on electrodes and I is total current flowing through the band then:

$$R_{\square} = \frac{U \cdot b}{I \cdot l} \tag{6}$$

One-sided graphite paper ($R_{\square} = 1.58 \cdot 10^3\ \Omega$) was used for building of analogous models for our analogous facility. Silver varnish Degussa 200 ($R'_{\square} = 0.4\ \Omega$) proved as the best for building of conductive parts of models edges (electrodes).

Measuring apparatus

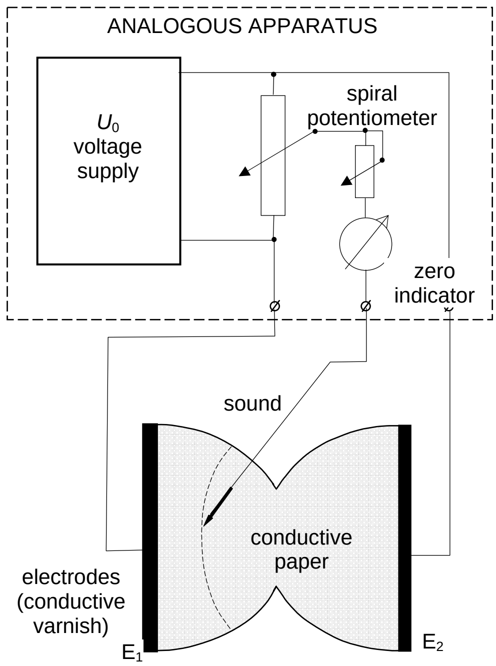

***Fig. 5** Analogous measuring apparatus*

The analogous apparatus (Fig. 5) consists of a controllable voltage supply fed on the model electrodes created on the graphite paper by high-conductive silver varnish. The 20-turn exact spiral potentiometer ARIPOT is used as specific redundancy. A scale of this device is of millesimal division and enables to set voltage on a rider with 0.1% resolution of total range of connected U_0 voltage. A micro-ampere meter of $\pm 5 \cdot 10^{-6}\,\mathrm{mA}$ range and resolution controlled by a serially connected potentiometer is used as a zero indicator [7]. A sound with a connective tip is connected with the indicator. In the model, it enables to find equipotential lines of the value set on the spiral potentiometer.

Results

1st Model: Contact of spherical particles

MAGNITUDES OF DC (DIRECT-CURRENT) RESISTANCES R, R_T AND R_A MEASURED BETWEEN E_1 AND E_2 ELECTRODES

Table 1

Measured values:							
Sample №	v	v (cm)	A (cm^2)	R (kΩ)	d (cm)	RT (kΩ)	R_A (kΩ)
1.1	0.1D	0.8	6.32	0.16	7.8	0.162	0.16
1.2	0.2D	1.6	12.64	0.32	7.7	0.328	0.32
1.3	0.3D	2.4	18.96	0.48	7.5	0.506	0.48
1.4	0.4D	3.2	24.89	0.63	7.2	0.702	0.65
1.5	0.5D	4.0	30.10	0.81	6.7	0.943	0.84
1.6	0.6D	4.8	36.40	0.96	6.3	1.203	1.00
1.7	0.7D	5.6	40.95	1.20	5.7	1.552	1.21
1.8	0.8D	6.4	44.03	1.58	4.5	2.247	1.47
1.9	0.9D	7.2	46.80	2.90	3.0	3.792	1.75

v – horizontal electrodes distance
D = 8 cm
d – overlay length (measured)
R – resistance measured on the models. It respects the electric field shape of samples for model 1.
R_T – transverse resistance between electrodes E_1 and E_2 without the constriction phenomenon influence (Eqn. (7))
R_A – average resistance corresponds to the resistance calculated at rectangular sample of the same length v and the same area as the model (Eqn. (8))
A – area of the sample (measured)

$$R_T = R_{\square} \cdot \frac{v}{d} \qquad (7)$$

$$R_A = R_{\square} \cdot \frac{v^2}{A} \qquad (8)$$

Nine samples of different d overlay lengths were created. R resistance is measured for each of them.

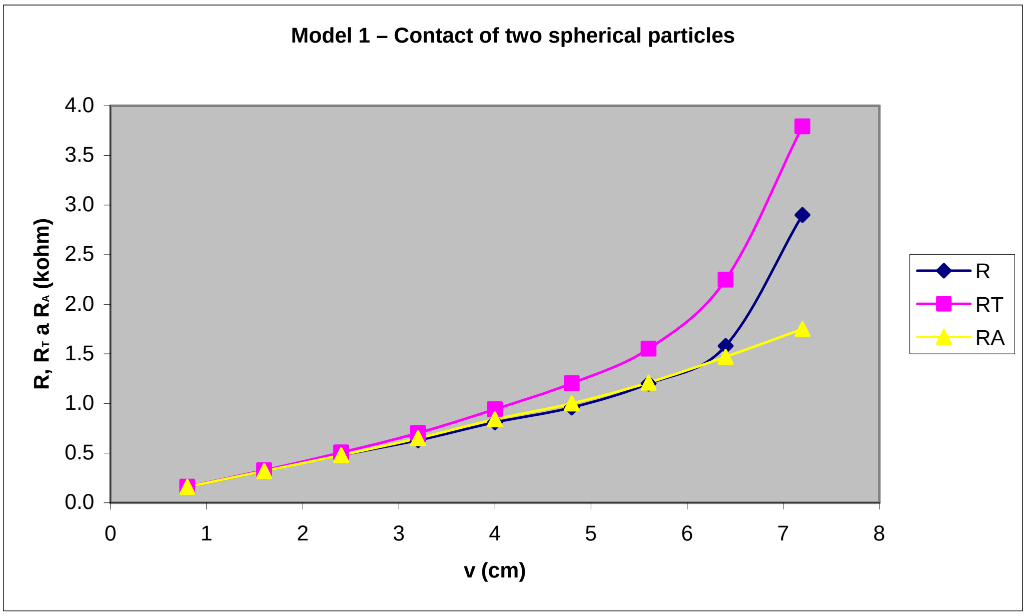

Fig. 6 *Resistances R, R_T and R_A measured between E_1 and E_2 electrodes as functions of the electrode distance v*

The electrical field on Fig. 7 and Fig. 9 is mapped by means of dimensionless equipotential lines frameworks $U^* = const$ and electrical streamline $W^* = const$ where W is so called current function. Dimensionless potential is standardized by $U_0 = U_2 - U_1$ difference of E_2 and E_1 electrodes. Then, a dimensionless potential value matches with $U = const.$ equipotential line.

$$U^* = \frac{U - U_1}{U_2 - U_1} \tag{9}$$

Electric streamlines form an orthogonal network to equipotential lines, i.e. stream density vector is tangential to streamlines. The current flowing between two streamlines is directly proportional to current functions difference. Like for potential, a dimensionless potential value matches with $W = const$ equipotential line

$$W^* = \frac{W - W_1}{W_2 - W_1}, \tag{10}$$

where W_1 and W_2 are values on P_2 and P_1 streamlines. Their difference is directly proportional to the total I current flowing between of E_2 and E_1 electrodes. 10% of total current flows between adjacent streamlines because W^* values on maps are chosen with $\Delta W^* = 0.1$ equidistant difference. Streamlines field is received in the inverse model where P_2 and P_1 streamlines are created as conductive electrodes and original E_2 and E_1 equipotential lines as non-conducting edges.

The electric fields in Fig. 7 and Fig. 9 were obtained by measuring in the analog model (Fig. 5) with conductive paper.

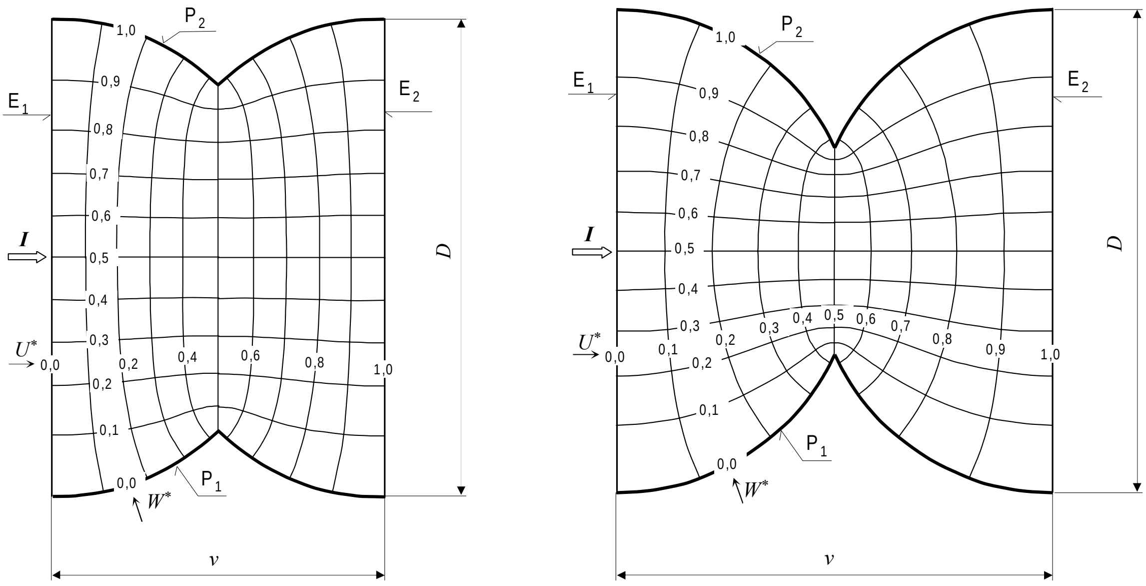

Sample № 1.7 Sample № 1.9

***Fig.** 7 Electrical fields on Model 1 samples*

It is possible to consider equivalency of the equipotential lines and the stream lines of solved 2-D model and of potential and current situation on the cross-section of two intergrowing spherical particles or spherical particles connected by cylindrical bridge. Conclusions of the 2-D modelling can be applied to the 3-D problems [4].

2nd Model: Connecting of two spherical particles by means of conductive bridge

MAGNITUDES OF DC RESISTANCES R, R_T AND R_A MEASURED BETWEEN E_1 AND E_2 ELECTRODES

Table 2

Measured values:							
Sample №	w (cm)	w/D	A (cm^2)	R (kΩ)	v (cm)	R_T (kΩ)	R_A (kΩ)
2.1	7.5	0.94	69.80	2.85	9.40	1.98	2.0
2.2	6.5	0.81	84.45	3.24	12.45	3.03	2.9
2.3	5	0.63	90.14	4.87	16.20	5.12	4.6
2.4	3	0.38	97.04	10.20	23.90	12.60	9.3
2.5	2	0.25	100.01	19.32	32.90	26.00	17.1

w/D – generalization (bridge width/particle diameter)
R – resistance measured on the models. It respects the electric field shape of the samples for model 2
R_T – transverse resistance between electrodes E_1 and E_2 without the constriction phenomenon influence (Eqn. (11))

$$R_T = R_{\square} \cdot \frac{v}{w} \tag{11}$$

Five samples with different *w* bridge width were created. *R* resistance is measured for each of them. The graph demonstrates exponentially decreasing dependence of *R* to *w*.

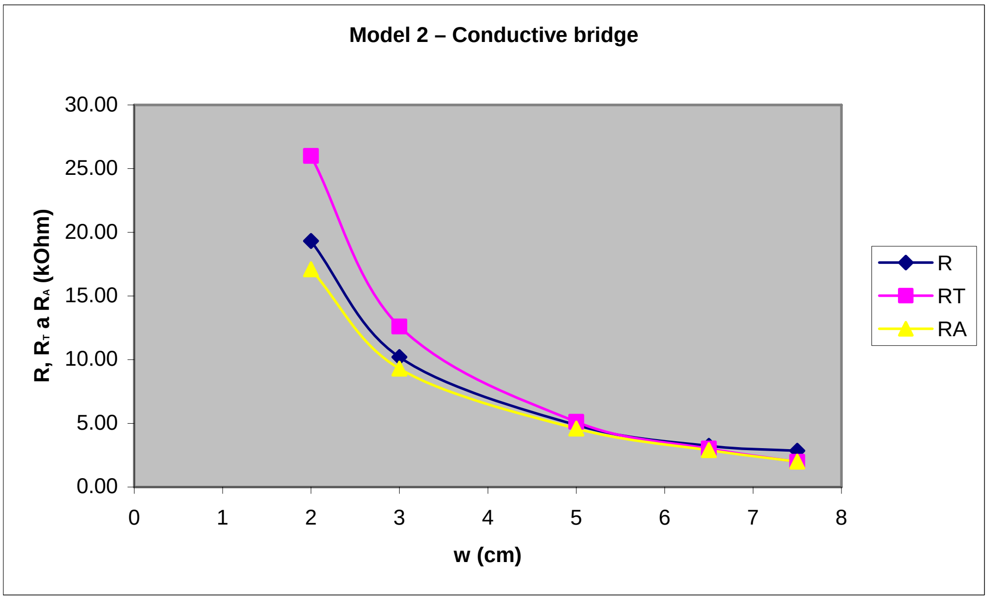

Fig. 8 *Resistances R, R_T and R_A measured between E_1 and E_2 electrodes as functions of the conduction path width w*

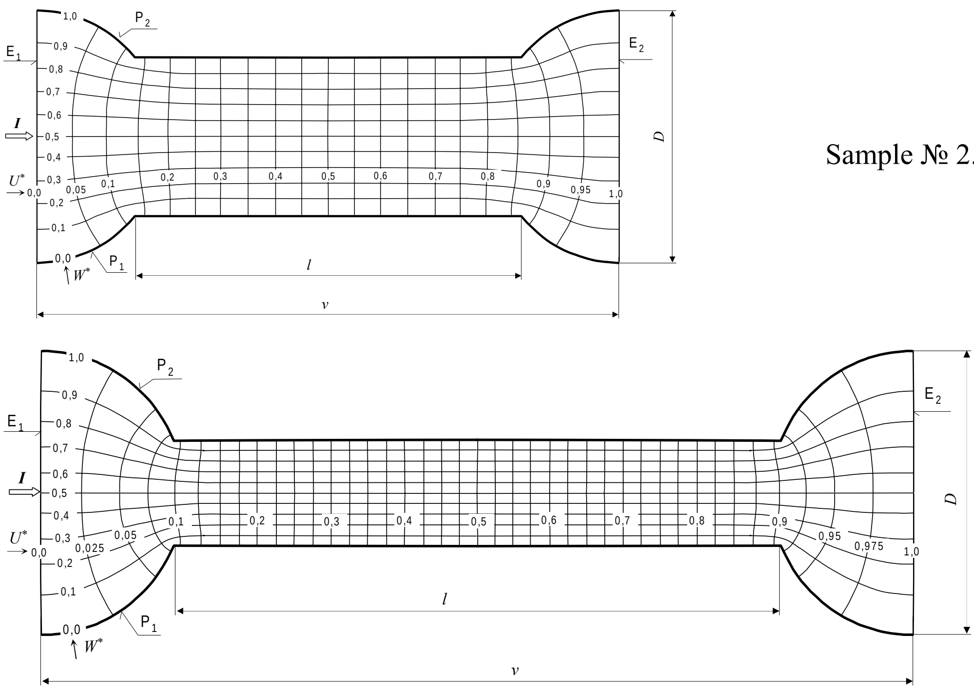

Sample № 2.3

Sample № 2.4

Fig. 9 *Electrical fields on Model 2 samples*

Conclusions

The two models of carbon particles connection show the electric field shape and electric resistance of the carbon particle/insulating matrix system.

It can be derived from the relations in Fig. 6 and Fig. 8 it:

1. The electric resistance of the system studied depends on the square resistance (resistivity) of the conductive component. But it is impossible to determine the composite resistivity only from the conductive component resistivity and its concentration even in the ideal clusters structure (without loops and dead ends). The constriction phenomenon influence is visible mainly at the high values of $\boldsymbol{v}$ and small values of $\boldsymbol{w}$ (see $\boldsymbol{R}$, $\boldsymbol{R_T}$ **and** $\boldsymbol{R_A}$ in Fig. 6 and Fig. 8). The constriction resistance is connected with non-homogeneous field at particles connections therefore the total composite resistance depends on the number of particles contact and on their junction resistance values.

2. The electric fields of some samples are in Fig. 7 and Fig. 9. The shape of equipotential lines and streamlines shows the current and the potential relative values of conductive clusters. The places with greatest current densities exhibit the greatest potential gradient and greatest local electric resistance. That fact influences calculated square resistance (resistivity) of the composite and non-homogeneous Joule heat evolving at certain current density also. From this follows that carbon particles of smaller diameter are more convenient for the low resistivity composites applications.

The study of the field deformation on the particles junction in the carbon particles/insulating matrix composite illustrates influence of constriction phenomenon on their electric and thermal properties.

References:

[1] WEBER, M., KAMAL, M.R. *Estimation of the volume resistivity of electrically conductive composites.* Polymer composites, Vol. **18** (1997), pp 711-725.

[2] THONGRUANG, W., SPONTAK, R. J. and BALIK, C. M. *Correlated electrical conductivity and mechanical property analysis of high-density polyethylene filled with graphite and carbon fiber.* Polymer Vol. **43** (2002), pp 2279-2286.

[3] MEINCKE, O. et all. *Mechanical properties and electrical conductivity of carbon-nanotube filled polyamide-6 and its blends with acrylonitrile/butadiene/styrene.* Polymer Vol. **45** (2004), pp 739-748.

[4] CINGERMAN, M.L. *Development and Modelling of Electrically Conductive Composite Materials,* Dissertation, Michigan Technological University 2001

[5] BALBERG I. et all. *Percolation and tunneling in composite materials.* International Journal of Modern Ph.B, Vol. **18** (2004), pp. 2091-2121.

[6] JIRKŮ, S. *Elektrická analogie složitějších hydrodynamických polí.* Písemná práce k odborné zkoušce ve vědecké přípravě, 1975.

[7] HOBZÍK, J. *Zařízení k analogovému řešení Dirichletovy okrajové úlohy v rovinném poli realizovaném vodivým papírem*. Diplomová práce, FEL ČVUT, 1971.